Saudi Pharmaceutical Journal 28 (2020) 791–802

Contents lists available at ScienceDirect

Saudi Pharmaceutical Journal

journal homepage: www.sciencedirect.com

Original article

Development and characterization of a superabsorbing hydrogel film containing *Ulmus davidiana* var. *Japonica* root bark and pullulan for skin wound healing

Tae Hoon Park [a,1], Sumi Lee [b,1], Reeju Amatya [a], Pooja Maharjan [b], Hye-Jin Kim [a], Woo Sung Park [a], Mi-Jeong Ahn [a], Sun Yeou Kim [c,d], Cheol Moon [e], Heesun Cheong [f], Kyoung Ah Min [b,*], Meong Cheol Shin [a,*]

[a] College of Pharmacy and Research Institute of Pharmaceutical Sciences, Gyeongsang National University, 501 Jinju Daero, Jinju, Gyeongnam 52828, Republic of Korea
[b] College of Pharmacy and Inje Institute of Pharmaceutical Sciences and Research, Inje University, 197 Injero, Gimhae, Gyeongnam 50834, Republic of Korea
[c] College of Pharmacy, Gachon University, 191, Hambakmoero, Yeonsu-gu, Incheon 21936, Republic of Korea
[d] Gachon Institute of Pharmaceutical Science, Gachon University, Yeonsu-gu, Incheon 21565, Republic of Korea
[e] College of Pharmacy, Sunchon National University, 255 Jungang-ro, Suncheon, Jeonnam 57922, Republic of Korea
[f] Division of Cancer Biology, National Cancer Center, 323 Ilsan-ro, Ilsandong-gu, Goyang, Gyeonggi-do 10408, Republic of Korea

ARTICLE INFO

Article history:
Received 26 February 2020
Accepted 28 May 2020
Available online 3 June 2020

Keywords:
Ulmus davidiana var. japonica
Root bark
Powder
Gel film
Wound healing

ABSTRACT

Ulmus davidiana var. *japonica* (UD) has widely been used in Korean traditional medicine for the treatment of various types of diseases including inflammation and skin wounds. The UD root bark powders possess gelling activity with an excellent capacity for absorbing water. This distinct property could make the UD root bark powders to be a great material for manufacturing a gel film specifically for the healing of large and highly exudating wounds (e.g., pressure sores and diabetic ulcers). In this research, we separated the UD root bark powder into 4 different samples based on their sizes and then tested their water absorption capacity and flowability. Based on these results, 75–150 μm sized and below 75 μm sized samples of UD root bark powders were chosen, and UD gel films were prepared. The UD gel films showed good thermal stability and mechanically improved properties compared with pullulan only gel film with excellent swelling capacity and favorable skin adhesiveness. Further, in the animal studies with the skin wound mice model, the UD gel films exhibited significant therapeutic effects on accelerating wound closure and dermal regeneration. Overall, this study demonstrated the applicability of UD root bark powders for hydrogel wound dressing materials, and the potential of UD gel films to be superior wound dressings to currently available ones.

1. Introduction

Wound healing is a multistep and complex process consisting of 1) inflammation, 2) proliferation, and 3) maturation phase (Hosgood, 2006). In the first inflammation stage, hemostasis and blood clot formation occur, during which immune cells are recruited and contribute to inflammation by the release of various cytokines and growth factors (Behm et al., 2012; Ridiandries et al., 2018). Next, in the proliferation stage, the cytokines and growth factors mediate re-epithelialization, extracellular matrix formation, and angiogenesis (Braiman-Wiksman et al., 2007; Raja et al., 2007). Lastly, wound contraction and remodeling occur in the maturation stage (Kao et al., 2011). These phases occur in an overlapping but well-ordered manner. To promote these wound healing phases, various wound dressings have been developed and used (Elzayat et al., 2018; Ustundag Okur et al., 2019). The major roles of wound dressings include 1) enhanced epidermal migration 2) promotion of collagen synthesis and angiogenesis, 3) protection against contamination (Dhivya et al., 2015). Recently, wet type occlusive dressings (generally hydrocolloid dressings) have been more popularly used than the traditional dry type dressings (Eaglstein, 2001; Phaechamud et al., 2019). However, these wet type dressings are not always adequate for every type of wound.

* Corresponding authors.
E-mail addresses: minkahh@inje.ac.kr (K.A. Min), shinmc@gnu.ac.kr (M.C. Shin).
[1] These authors contributed equally.

Peer review under responsibility of King Saud University.

Production and hosting by Elsevier

https://doi.org/10.1016/j.jsps.2020.05.007
1319-0164/

In the case of highly exudating large wounds or neuropathic ulcers, wound dressings that could effectively dry the exudates may be more beneficial (Ovington, 2007; Seaman, 2002). Specifically, for these wounds, an ideal dressing may include the following properties: 1) thin but possessing adequate mechanical strength to maintain the structure, 2) high capacity for absorbing large exudates, and 3) ease of removal after absorbing the exudates.

Ulmus davidiana var. *japonica* (UD) is distributed in many Asian countries including Japan and Korea. It is a member of the elm family that is most popular by the slippery elm (*Ulmus rubra*) which is a native tree in North America. According to Watts et al, the slippery elm bark is mainly composed of various fibers (that include insoluble cellulose, hemicellulose, lignin, and soluble mucilage) and tannins (Watts and Rousseau, 2012). For UD elm barks, along with those, various bioactive components (e.g., lignin derivatives, catechin derivatives, flavonoids, phenolic compounds, etc.) have been reported (Jung et al., 2008; Lee et al., 2008). Because of these components, the UD extracts have long been used as Korean traditional medicine to treat inflammatory and gastroenteric disorders (Lee et al., 2001; So et al., 2019). Also for external use, the extracts have widely been used for ulcers, cold sores, boils, and abscesses. The main component responsible for the above medicinal usage is the mucilage that endows the UD bark powders unique physical properties of excellent swelling and gelling ability (Kang et al., 2020). The mucilage is large and highly branched polymers composed of different types of sugars and uronic acids coupled by glycosidic bonds (Watts and Rousseau, 2012). In our previous study, when the UD root bark powder was topically applied to the wound site in the animal model, it absorbed the exudates and swelled to form a viscous gel that could cover the wound and prevent further infection (Kang et al., 2020). Despite the therapeutic potentials of the UD root bark for topical wound healing, powder may not be a favorable type of pharmaceutical formulation when compared to the film type dressings. However, to date, there have been no reports of development of any UD gel formulation made up of the original root bark.

Pullulan (also referred to as α-(1 → 6) linked maltotriose), is a natural homopolysaccharide primarily produced by the strains of fungus, Aureobasidium pullulans (Leathers, 2003). It possesses a linear structure composed of interconnected maltotriose units by α-1,6 glycosidic bonds. In the maltotriose, 3 glucose units are linked by α-1,4 glycosidic bonds. This distinctive connection pattern of pullulan provides excellent film-forming ability with structural flexibility, adhesive properties, and strong mechanical strength (Leathers, 2003; Vuddanda et al., 2017). Despite the higher price than synthetic polymers, pullulan possesses great advantages such as low toxicity, low mutagenicity, edibility, biodegradability, and high water solubility (Han and Lv, 2019). Most of all, pullulan can form thin films with great mechanical properties (Pathare et al., 2013). In this research, to effectively utilize the favorable properties of UD root bark, we formulated a UD root bark and pullulan-containing hydrogel film for wound healing. The prepared UD gel film was investigated for its thermaland mechanical properties, and the therapeutic efficacy was assessed in a mouse wound model. Macroscopic imaging and histological analyses were employed for evaluating the healing effects.

2. Material and methods

2.1. Materials

Pullulan, glycerin, absolute ethanol, xylene, paraffin, and formalin solution were purchased from the Sigma-Aldrich Co. (St. Louis, MO, USA). For tissue staining, Harris hematoxylin and Eosin Y reagents were obtained from YD Diagnostics (Yongin, Republic of Korea) and Muto Pure Chemicals Co. (Tokyo, Japan), respectively. VectaMount mounting solution was purchased from Vector Laboratories, Inc. (CA, USA). Slide glass and coverslips were obtained from ThermoFisher Scientific, Inc. (MA, USA). The Masson's trichrome stain kit was obtained from Abcam (Cambridge, UK).

2.2. Preparation of Ulmus davidiana var. Japonica (UD) root bark powders

Pulverized powders of the root barks of *Ulmus davidiana* var. *japonica* (UD) (provided by Prof. Mi Jeong Ahn, Gyeongsang National University, Republic of Korea) were separated into 4 different particle sizes by using 18, 50, 100 and 200 mesh sieves (pore sizes are 850, 300, 150 and 75 μm, respectively). The powder samples will be classified based on their particle size ranges separated by the sieving as 1) 300 – 850 μm (in diameter)-, 2) 150 – 300 μm (in diameter)-, 3) 75 – 150 μm (in diameter)-, and 4) below 75 μm (in diameter)-sized samples. The optical and scanning electron microscopic (SEM) images of the powder samples are shown in Figure S1.

2.3. Characterization of the UD root bark powder samples

The properties of UD root bark powder samples with different particle size ranges (300 – 850 μm, 150 – 300 μm, 75 – 150 μm, and below 75 μm sized samples) were characterized. First, the morphology and size of the powder samples were examined using SEM. As shown in Figure S1B, the particle size differences in the samples were clearly observed, and, with the particle size getting smaller, the shape was found more homogenous and round. Next, the water absorption capacities of the powder samples were determined by following the protocols described by Yang et al. with modifications (Yang et al., 2010). Briefly, 10 mg (W_{sample}) of powder samples were added to 1 mL of double-distilled water (DDW) in Eppendorf tubes and then weighed the tubes (W_{total}). The samples were incubated at 37°C for 30 min and then centrifuged for 10 min at 12,000 rpm. The supernatant was carefully removed, and the supernatant was weighed (W_{spnt}). The water absorption capacities (Wc) of the UD root bark powder samples were calculated by using the following equation: $Wc = (W_{total}-W_{spnt}-W_{sample})/W_{sample}$. The flowability of the samples was determined by measuring the angles of repose (θ). Briefly, a funnel was fixed above 30 cm (H) and the powder samples were poured through the funnel until the apex of the formed powder cone reaches the bottom tip of the funnel. The mean diameter (2R) of the powder cone was measured and the angle of repose (θ) was calculated by using the following formula: $\theta = \tan^{-1}(H/R)$. The bulk and tap densities of the powder samples were measured by using a 10 cm mass cylinder. Briefly, a certain amount of weighed powder samples were poured into the cylinder, and the volume was measured (for bulk density measurement). One hundred taps were then administered, and the volume was again measured (for tap density measurement). The Hausner's ratio was calculated by dividing the tap density by bulk density. The Carr's compressibility index (CI) was calculated by the following equation: CI = 100(1-bulk density/tap density).

2.4. Preparation of hydrogel films containing UD root bark powder (UD gel film)

UD gel films containing UD root bark powder samples were formulated using pullulan as the co-gelling agent and glycerin as the plasticizer (Table 1). Briefly, 0.5 g pullulan was dispersed in 20 mL of DDW by stirring at 37 °C and, after then, 0.75 g of glycerin was added. To the pullulan/glycerin mixture, the UD root bark powder sample was added, and, after thorough mixing by vortexing, the gel

Table 1
Formulation table for hydrogel films containing Ulmus davidiana var. japonica (UD) root bark powder.

Gel Film Formulation [a]	Pullulan (g)	Glycerin (g)	UD Root Bark Powder	
			Sample Type	Content (g)
Gel Film-1	0.5	0.75	100–200 mesh	0.25
Gel Film-2	0.5	0.75	100–200 mesh	0.5
Gel Film-3	0.5	0.75	100–200 mesh	1.0
Gel Film-4	0.5	0.75	200 mesh	0.25
Gel Film-5	0.5	0.75	200 mesh	0.5
Gel Film-6	0.5	0.75	200 mesh	1.0

[a] Above compositions were dispersed in total 20 mL of DDW and then dried.

was spread onto a 100 mm diameter petri dish, followed by drying at 50 °C incubator for overnight to form a hydrogel film.

2.5. Morphological change of gel films before and after water absorption

Dried UD (Gel Film-2) and pullulan gel films (average weight: 80 (±6) mg, size: 2 cm × 2 cm) were placed in a petri dish and then DDW was added to the gel films. The images of the gels were acquired before and after water absorption. After the gels were dried, their gel images were taken again.

2.6. FT-IR analysis

The infrared spectra of pullulan, UD root bark, control gel film, and the UD gel film (Gel Film-2) were acquired at the wavelength range of 400 – 4,000 cm^{-1} using an FT-IR microscope (VERTEX 80v, Bruker, Billerica, MA, USA).

2.7. Thermogravimetric analysis (TGA)

The TGA was carried out for dried pullulan, UD root bark, pullulan gel film, and the UD gel film (Gel Film-2) using the thermogravimetric analyzer (TGA Q500, TA Instruments, New Castle, DE, USA). The measurement was carried out in the temperature range of 25–600 °C at a heating rate of 10 °C/min under nitrogen atmosphere. The thermogravimetric (TG) and differential thermogravimetric (DTG) curves were acquired using the TGA software (Universal V4.5A TA Instruments).

2.8. Dynamic mechanical thermal analysis (DMTA) of the UD gel film

DMTA of the UD and pullulan gel films were carried out using a dynamic mechanical analyzer (DMA Q800, TA Instrument). The measurement was performed on the samples by tension mode, at a frequency of 1 Hz, amplitude of 20 μm, a temperature range of −30 – 100℃, and a heating rate of 5℃/min.

2.9. Tensile strength of gel films

The tensile strength of the pullulan gel film and UD gel film was measured using a universal testing machine (Instron 3367, Instron Corporation, Norwood, MA, USA). The gel film samples were prepared according to ASTM D882. The crosshead speed was set for the pullulan gel film and the UD gel film at 500 mm/min and 12.5 mm/min, respectively. For comparison of the mechanical properties of Gel Film-2 and Gel Film-5, the maximum elongation at break and tensile strength were determined by using Texture Analyzer (Brookfield CT3 Texture Analyzer, Brookfield Engineering Laboratories, Middleboro, MA, USA)). For the measurement, UD gel films (Gel Film-2 and Gel Film-5) were prepared in square shapes (length: 25.4 mm, width: 25.4 mm and thickness: average 300 μm) and were held between 2 clamps. The films were pulled at the crosshead speed at 0.5 mm/min and the % elongation and tensile strength at break were measured.

2.10. Swelling kinetics

The swelling properties of the UD gel film (Gel Film-2) were determined by immersion of the dried gels (average weight: 80 (±6) mg, size: 2 cm × 2 cm) in simulated wound solutions (adjusted pH to 2.0, 7.4, or 9.2) at 37 °C. The recipe of the simulated wound solutions was adopted from Bradford et al (Bradford et al., 2009). At pre-determined time points (0, 15, 30, 45, 60, 120, 240, 360, 1440 min), the swollen hydrogels were removed (n = 3), and weighed after blotting the excess water on the surface. The swelling ratio (Qs) was calculated by dividing the weight of the gels in the wet state by the initial gel weights in the dried state. Also, to compare the swelling capacity of different gel film formulations (Gel Film-1–6), additional swelling studies were carried out using simulated wound solutions at pH 7.4 with incubation for 1 h, and the Qs values of the gel films were calculated.

2.11. Bioadhesiveness study of the UD gel films

The bioadhesive forces of the UD gel film formulations (Gel Film 1 – 6) and commercial Mediderm dressing were determined by using Texture Analyzer (Brookfield CT3 Texture Analyzer, Brookfield Engineering Laboratories, Middleboro, MA, USA). The study was performed following the reported procedures with modification (Nayak et al., 2014). Briefly, the UD gel and Mediderm samples (3 cm × 3 cm) were attached to the upper probe, and pig skin (4 cm × 4 cm) was attached to the lower probe using adhesive bands leaving (3 cm × 3 cm) space for the sample binding. For the wet skin condition, a small amount of water was added to the surface of the pigskin just before the study. The texture analyzer was armed with a 10 kg load cell. The upper probe was moved downward until the samples were in contact with the pigskin at a constant force of 0.01 N. After maintaining the force for 60 s, the probe was lifted upwards at 0.1 mm/s. The peak detachment force (N) required to detach the samples from the pigskin was measured.

2.12. Cell culture

Detroit 551 human normal skin and B16F10 murine melanoma cell lines were purchased from the Korean cell line bank (Seoul, Republic of Korea). Both the cells were cultured in DMEM medium containing 10% FBS (with 1% antibiotic antimycotic & 1% penicillin–streptomycin) and the cell culture was maintained in a cell incubator (5% CO_2) at 37 °C.

2.13. Cytotoxicity assay

Cytotoxicity studies were carried out following the procedures by Makarand et al with modification (Risbud and Bhonde, 2000).

Briefly, the UD gel films were incubated in 10 mL of DMEM (final 5 mg/mL) at 37 °C for a total of 15 days. The extract was filtered through a 0.22 μm filter and then the cytotoxicity of the leach-out products was tested on Detroit 551 cells (human normal skin cells) and B16F10 (murine melanoma) cells. Briefly, both the cells were seeded onto 96-well plates (cell density: 10^4 cells per well) and, after overnight incubation, the cells were treated with a varying concentration (0–50%) of the gel extracts for 24 h at 37 °C in the cell incubator. After incubation, the cell viability was determined by WST-1 assay following the manufacturer's protocol (iNtRON Biotechnology, Daejeon, Republic of Korea).

2.14. Hemolysis assay

The hemolysis assay was carried out following the protocol described by Hussain et al with modification (Hussain et al., 2016). Briefly, blood was collected from ICR mice by cardiac puncture under anesthesia and added to heparinized tubes (BD Vacutainer® sodium heparin tubes). After then, the mouse plasma was dispensed to Eppendorf tubes (100 μL per tube) and the red blood cells (RBCs) were prepared by centrifugation (at 3000 rpm for 15 min) of the blood. After washing the RBCs with phosphate buffer saline (PBS; pH 7.4), 450 μL of PBS was added to the RBC suspension (to a final RBC concentration of 10% (v/v)), followed by addition of the UD gel film (weight: 5(±0.3) mg, size: 0.5 cm × 0.5 cm) or 1% (v/v) Triton-X 100 (as positive control). The samples were incubated for 24 h at 37 °C. After incubation, the samples were centrifuged (3000 rpm for 10 min) and the absorbance at 540 nm of the supernatants was measured for determination of the released extent of oxyhemoglobin (Oxy-Hb).

2.15. Animal model

ICR mice were purchased from Koatech (Gyeonggi-do, Korea) and acclimated for 1 week before the study. Mice were randomly divided into 4 groups (N = 6): 1) control, 2) control gel film (containing no UD root bark powder), 3) UD gel film and 4) Madeca Band® (positive control; a commercial hydrocolloid wet dressing film containing natural herbal extracts product purchased from a local pharmacy). For each mouse, two wounds were inflicted by using a 10 mm diameter biopsy punch at their posterior dorsal site.

2.16. Wound treatment

The gel samples were topically applied to the wound every day for a total of 5 days after cleaning the wound with povidone-iodine disinfectant solution. For the control group, only the povidone-iodine solution was treated. After wounding, the wound size was measured every day by taking the images with a digital camera and analyzing it by using Image J software (NIH, Bethesda, MD, USA). On Day 6, the mice were sacrificed, and the skin of the wound area including the normal tissue near the wound was harvested and immediately fixed in 10% formalin. The tissue specimens were embedded in paraffin and sectioned. After then, the samples were stained with hematoxylin and eosin (H&E) and further with Masson's trichrome according to the manufacturer's instructions (Kim et al., 2019).

2.17. Statistical analysis

All data are presented as mean ± standard deviation. The statistically significant difference of the data was analyzed by using 1-way ANOVA with Tukey's multiple comparison test as the post hoc test. Data with $p < 0.05$ was considered significant.

3. Results and discussion

3.1. Properties of UD root bark powder samples

Wound healing is a stepwise complex process (Braiman-Wiksman et al., 2007; Raja et al., 2007). The primary purposes of wound dressings are to accelerate the wound healing time as well as prevent potential opportunities for any infection (Yeo et al., 2019). For common wounds, recently, wet dressings including foam and hydrocolloid dressings have been popularly used, as they could allow healing without forming a scab over the wound by keeping the fluids from the wound under the dressings and maintaining the wound area moist (Bishop et al., 2003; Dabiri et al., 2016; Kannon and Garrett, 1995). Despite these advantages, however, specifically for relatively large wounds which have a large amount of fluids weeping, such as bedsore and diabetic foot ulcer, wet dressings may not be the optimal choice. This is because, for this purpose, it would be more beneficial to initially remove a large part of the fluids from the wound rather than keeping them under the dressings. In this regard, UD root bark powders could be considered a great choice as a material for such dressings. This is because, as shown in Figure S2, UD root bark powders possess the gelling activity and could absorb a high capacity of water (Lai and Rogach, 2017). When compared with the extract of UD root bark which showed almost no water absorption ($W_{water}/W_{UD\ root\ bark\ powder}$ of extract: 1.3), all the UD root bark powder samples showed a great capacity of water absorption. Among the UD root bark powder samples, specifically, samples with the size ranges of 150 – 300 μm and 75–150 μm samples showed markedly higher water absorption ($W_{water}/W_{UD\ root\ bark\ powder}$ of 150 – 300 μm and 75–150 μm sized samples: 85.1 and 87, respectively), in comparison with 300–850 μm and below 75 μm-sized samples ($W_{water}/W_{UD\ root\ bark\ powder}$ of 300–850 μm and below 75 μm-sized samples: 21.9 and 31.2, respectively). The lower water absorption capacity of the below 75 μm-sized samples could be explained by its low dispersibility, as the finest powders tended to readily aggregate in water and got limited access to the water molecules.

The flowability of the powder samples was determined by measuring the angle of repose, bulk density, tapped density, Hausner ratio (HR), and Carr's compressibility index (CI) (Patil et al., 2019; Son et al., 2019). The data are summarized in Table S1. As seen, the angles of repose for the samples, except for the 300 – 850 μm sized sample, are in the range of 46 – 55°, indicating that the flow is rated as 'poor which must be agitated or vibrated'. The angle of repose for the 300 – 850 μm sized sample is higher than 56°, indicating 'very poor' flow. Regarding the HR and CI, which are measures of powder bridge strength and inter-particulate friction, respectively, CI > 38 or HR > 1.60 is considered 'very very poor' flow. As seen from Table 1, except for the 150 – 300 μm sized sample, all the samples belong to this category. For the 150 – 300 μm sized sample, as the CI and HR are within 32–37 and 1.46–1.59, respectively, it is considered to have a 'very poor' flow. Overall, the flowability data indicated that, regardless of the particle size, UD root bark powder samples similarly possessed very poor flowability. Based on the water absorption and flowability study results, we have chosen to prepare gel films with 75 – 150 μm sized and below 75 μm sized powder samples, respectively, as they possess similar flowability but could stand for samples with higher and lower water absorption capacity.

3.2. Preparation of UD gel films

For the preparation of hydrogel films, pullulan and UD root bark powders were used as the gel matrix (Table 1) and glycerin was added as the plasticizer. Glycerin could provide softness and

flexibility to the gel film (Ma et al., 2017). Around 1:0.5 ~ 0.7 wt ratio was adequate for gel matrix-to-glycerin. Above the ratio, the gel film became too sticky and was difficult to detach from the petri dishes. Preliminary trials suggested that the maximum available concentration of pullulan was close to 5% (w/w). At pre-determined concentrations of UD root bark powders (0.25 – 1.0 g dispersed in 20 mL DDW), the mixture of pullulan, glycerin, and UD root bark powders showed good miscibility to create a uniform hydrogel network (Table 1, Fig. 1). The film casting method was adopted for the preparation of gel films because of simplicity, inexpensiveness, and relative ease for preparation in the laboratory. When the prepared gel films were dried, they could be easily detached from the petri dishes. As shown in Fig. 1, the appearance of the gel films was brownish in color and relatively uniform. The scent of the UD root bark was preserved in the gel films and, the films showed a slightly rough surface (Fig. 1). The SEM images of the UD gel films showed a rougher surface with an increasing amount of UD root bark powder samples (Figure S3). With the given recipe, when the UD root bark only gel film was too brittle for further use, while the pullulan gel film could be successfully prepared.

3.3. Morphological change of gel films with water absorption

Fig. 1 is showing the images of the UD and the pullulan gel films. The pullulan gel film was readily dissolved in DDW within 30 min, while the UD gel film kept maintained its structure throughout the study. In the water, the swelling was observed from the UD gel film after immersion, but, after getting dried, the morphology was similar to the initial shape before water absorption. These results indicated the possible presence of interconnection of the mucilage of UD root bark powder and the pullulan polymers.

3.4. FT-IR spectra of pullulan, UD root bark, pullulan gel film, and the UD gel film

The FT-IR spectra of pullulan, UD root bark, control gel film, and UD gel film (Gel Film-2) are shown in Fig. 2. As seen, characteristic peaks of pullulan are observed from both the pullulan and UD gel films. The peaks at 3288 and 2927 cm^{-1} are attributed to the stretching vibrations of OH and CH/CH_2, respectively (Chen et al., 2017). The peak at 1355 cm^{-1} is assigned to CH/CH_2 deformation vibration and the peak at 1150 cm^{-1} stands for the vibrations of "C-O-C" and glycosidic bonds (Chen et al., 2017; Zhang et al., 2013). The peak at 1019 cm^{-1} is attributed to C-OH bending vibration (at the C6 position) (Zhang et al., 2013). The peaks of 923 and 850 cm^{-1} evidenced the presence of α-(1,6) glycosidic bonds and the α-glucopyranoside units, respectively (Chen et al., 2017). From the UD gel film, the distinctive peak observed from the UD root bark was also observed (1603 cm^{-1} attributed to C = O asymmetric stretching) (Archana et al., 2013). Collectively, the FT-IR data indicated the incorporation of both the pullulan and UD root bark components in the UD gel film. Furthermore, the data also showed the presence of many hydrophilic groups (hydroxyl and carboxyl groups) in both the pullulan polymer and the UD root bark (including mucilage) that could allow the formation of hydrogen bonds among them, leading to the cross-linked gel film formation.

3.5. TGA

TGA is a useful tool to assess the thermal stability of polymeric materials (Gałka et al., 2014). As shown in Fig. 3, pullulan, UD root bark, pullulan gel film, and the UD gel film (Gel Film-2) were analyzed by TGA at a heating rate of 10 °C/min. In the case of pullulan, a single sharp peak was observed from the DTG curve at 317.32 °C

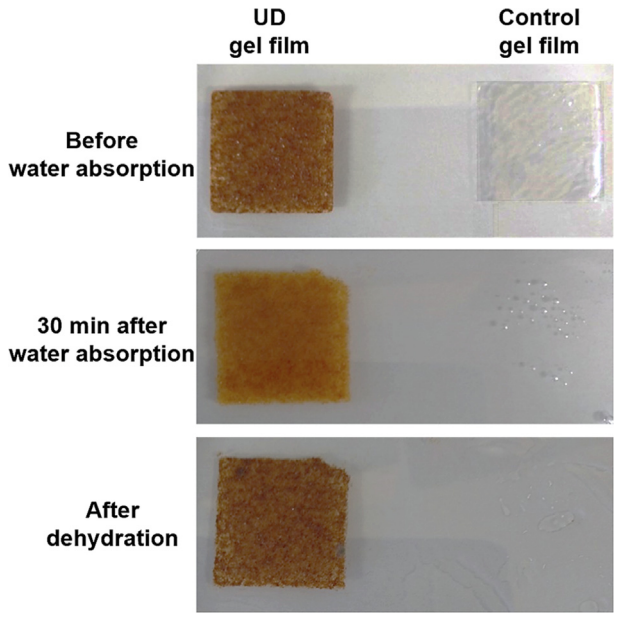

Fig. 1. Optical images of UD gel film and pullulan gel film before and after water absorption.

indicative of its main degradation temperature (Fig. 3A). This result was similar to the data (295 °C by differential scanning calorimetry) reported by Teramoto et al (Teramoto and Shibata, 2006). The UD root bark showed relatively broad TG and DTG curves with 2 main degradation temperatures at 288 and 347.71 °C (Fig. 3B). It was also found that by 183 °C, 10% weight loss was observed which may be explained by the evaporation of water possibly adsorbed on the surface of the powders (Kavousi et al., 2017). This suggested the hygroscopic properties of the UD root bark. Similarly, the pullulan gel film and the UD gel film also showed 10% weight loss by 188 and 177 °C, respectively (Fig. 3C and 3D). For the pullulan gel film, the DTG curve showed a multi-step degradation at around 198.8 to 319.6 °C that continued until 600 °C with a total of 90% weight loss (Fig. 3C). The early peak at 198.8 °C may exhibit the degradation of glycerin incorporated in the gel film (Xu et al., 2017). The UD gel film revealed a broader TG curve than the pullulan gel film and 3 main peaks (at 212.4, 269, and 312.5 °C) were observed from the DTG curve (Fig. 3D). The peak at 212.4 °C likely shows the glycerin degradation, and the accumulated weight loss until 600 °C was 81.3%, which was slightly less than the pullulan gel film. Overall, the TGA results suggested that the overall thermal stability of the UD gel film is lower than the pullulan gel film. However, at temperatures below 177 °C, 90% of both the gel films could maintain their stability.

3.6. DMTA of the UD gel film

For the gel films, possessing desirable mechanical properties to maintain structural integrity would also be crucial to protect the wound region from oxygen and infection. DMTA is a useful technique to evaluate the thermomechanical properties of polymers and gels (Jones, 1999). Specifically, the DMTA is an optimal tool for assessing the viscoelastic properties of materials to an oscillating force (stress) as a function of temperature. Fig. 4 shows the temperature-dependent profiles of storage modulus, loss modulus, and tangent delta of the pullulan gel film and the UD gel film. As seen from Fig. 4A, for the pullulan gel film, storage modulus values were higher than the loss modulus up to 50 °C, indicating the predominant elastic property of the gel film below 50 °C. However, the

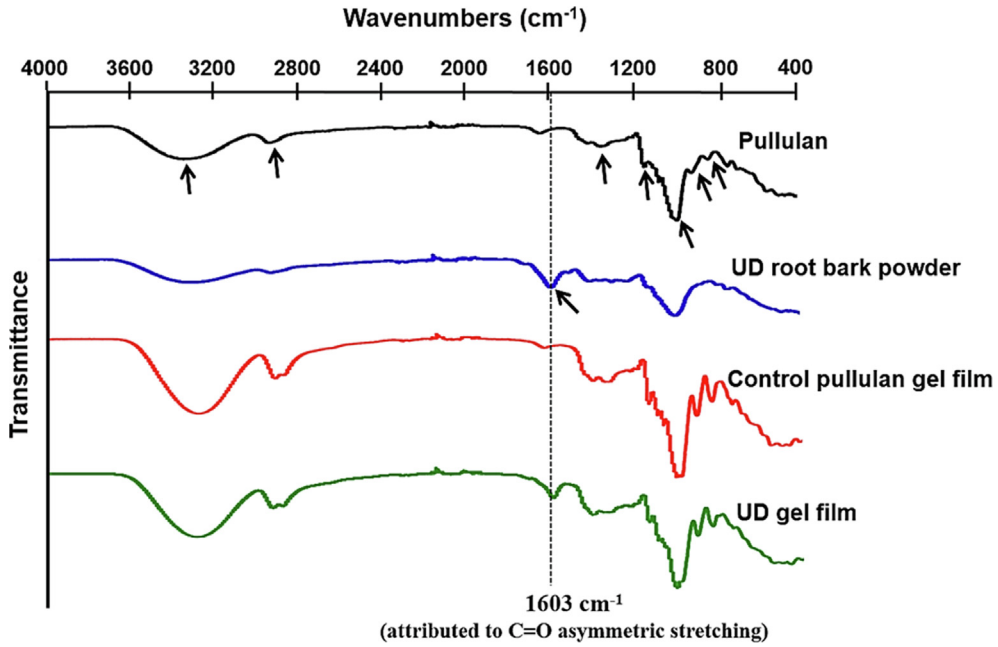

Fig. 2. FT-IR spectra of pullulan, UD root bark, pullulan gel film, and UD gel film (Gel Film-2).

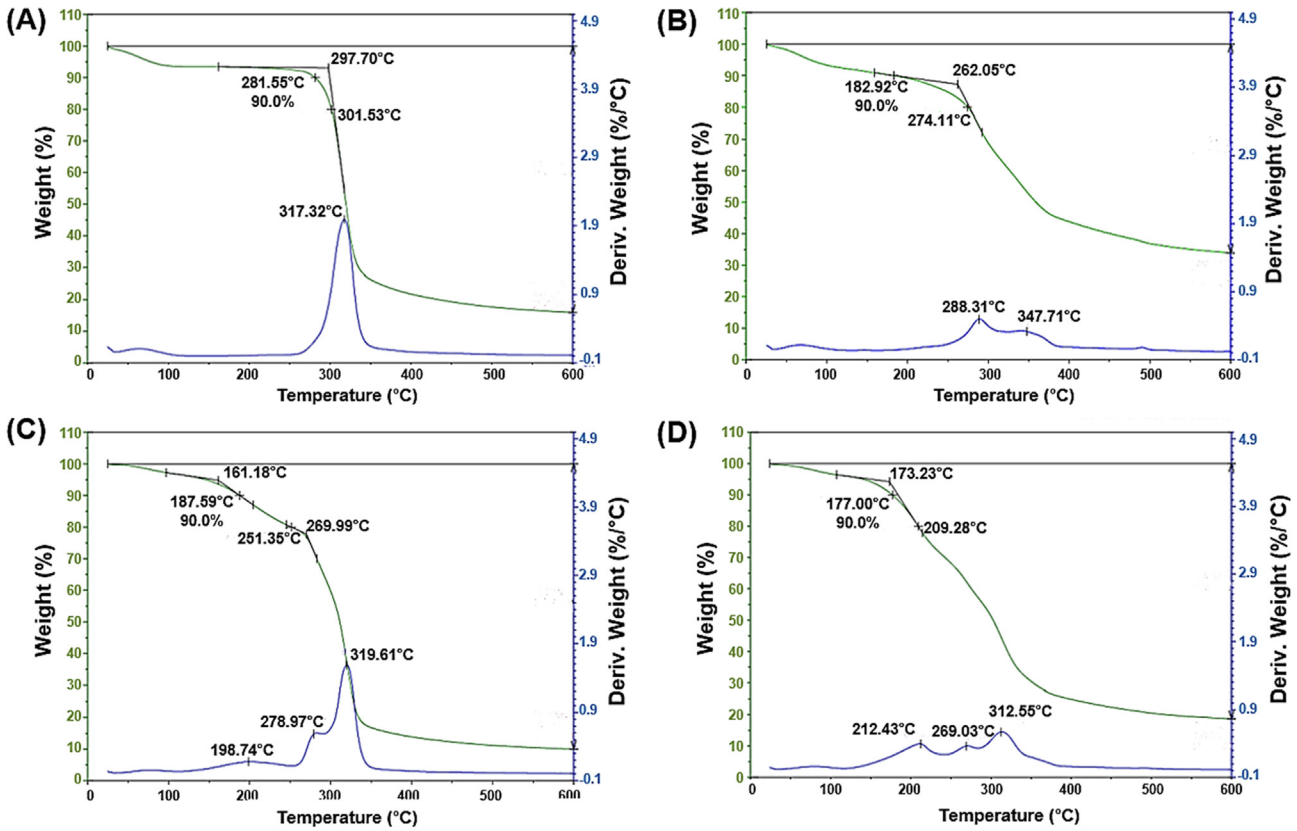

Fig. 3. Thermogravimetric analysis (TGA) of (A) pullulan, (B) UD root bark, (C) pullulan gel film, and (D) UD gel film (Gel Film-2). The measurement was carried out in the temperature range of 25–600 °C at a heating rate of 10 °C/min under nitrogen atmosphere.

glass transition occurred as low as 15.6 °C (1st peak of the tangent delta curve); possibly due to the excessively high contents of glycerin (50% of the pullulan weight) in the gel film used as the plasticizer. Related to this finding, Vuddanda et al reported the plasticizer effects on the Tg for the pullulan gel films (Vuddanda et al., 2017). With the glycerin content increasing from 0 to 30%, the Tg value significantly decreased from 222 °C to 74 °C. From above 30 °C, the tangent delta value sharply risen; suggesting that the sample is becoming less hard and more flexible. After reaching 55 °C, the gel appeared to transit to the viscous region and became

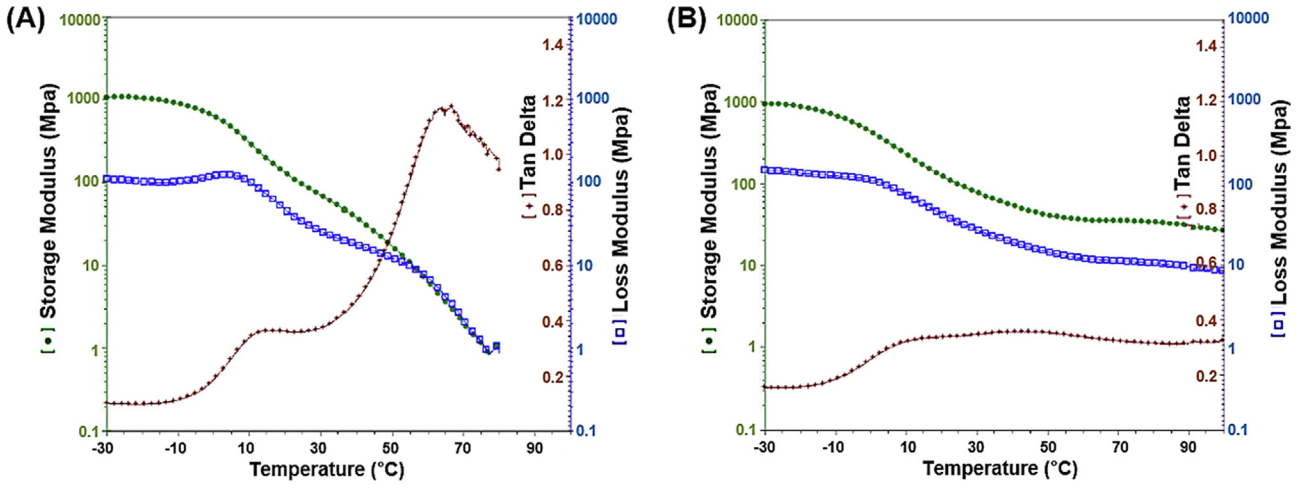

Fig. 4. Dynamic mechanical analysis of the (A) pullulan gel film and (B) UD gel film (Gel Film-2).

fluidic. The 2nd peak of the tangent delta at 66.5 °C appeared to correlate with the Tg of glycerin (reported to be 70.5 °C by Li et al) (Li et al., 2008). Compared to the pullulan gel film, the UD gel film showed sharply different DMTA results. As shown in Fig. 4B, while the pullulan gel film melted around 55 °C, the UD gel film did not flow at temperatures up to 100 °C; evidencing the presence of a more significant level of crosslinking (Collins and Birkinshaw, 2008). Also, a much broader transition was observed in the temperature range of 10–50 °C. This might be explained by the inhomogeneity of the UD gel film likely due to the immiscible compositions (e.g. water-insoluble fibers) of the UD root bark incorporated into the gel film (Watts and Rousseau, 2012).

3.7. Tensile strength of gel films

Tensile strength represents the mechanical property of the gel film to resist break on elongation. The % Elongation is the change in the original length before breaking and shows the extensibility of the formulation (Sezer et al., 2007). Tensile strength stands for the highest tensile stress sustained by the samples. The stress–strain curves of the pullulan gel film and the UD gel film are shown in Fig. 5. As seen, the pullulan gel film (Fig. 5A) showed a tensile strength of 0.22 N/mm^2, and the UD gel film (Fig. 5B) had a 2-fold higher value (0.38 N/mm^2). It was previously reported that the contents of plasticizers would negatively correlate with the tensile strength of gel films. According to Vuddanda et al, the tensile strength of pullulan gel films with 10 – 30% glycerin contents were in the range of 0.5 – 6 N/mm^2 (Vuddanda et al., 2017). Therefore, the relatively low tensile strength of both the tested gel films may be explained by the high (50%) glycerin contents.

The comparison of the tensile strengths of 2 UD gel films (Gel Film-2 and Gel Film-5) are shown in Table 2. As seen, compared with Gel Film-5, the Gel Film-2 had significantly greater tensile strength. The results suggested that the particle size of UD root bark powders could significantly affect the interaction among the polymers that contribute to the gel film strength.

3.8. Swelling study

To become a good dressing specifically for large wounds, as aforementioned, it is of most importance for the wound dressing to absorb a large amount of exudate (Adderley, 2010). Therefore, the swelling behaviors of the prepared gel films were investigated. Fig. 6 shows swelling kinetics of the UD gel film in the simulated wound solutions at different pH of 2, 7.4, and 9.2. As seen in Fig. 6A, swelling occurred rapidly within 1 h and then gradually plateaued at around 6 h. The UD gel film attained high swelling ratios of 11.4, 16.5, and 28.9 after 6 h of swelling (when reached the plateau) in pH 2, 7.4, and 9.2 solutions, respectively. The extent of swelling of the UD gel film was highly dependent on the pH. At low pH (pH 2), the extent of swelling was lower than the neutral and basic environment; presumably due to reduced electrostatic repulsion by protonation of acids (e.g., uronic acids contained in the mucilages of the UD root bark) (Watts and Rousseau, 2012). On the other hand, at basic pH (pH 9.2), the extent of swelling was significantly (1.8-fold at 24 h; Qs of 18.5 vs. 32.5) higher than at pH 7.4. As the pullulan and glycerin only possess –OH groups, the pH-dependency of the swelling kinetics of the UD gel film are likely caused mainly by the acidic constituents of the UD root bark.

As seen from Fig. 6B, when the swelling capacity of the UD gel films were compared, they all showed a significantly greater extent than the commercial Mediderm® hydrocolloid dressing. Among the prepared gel films, those composed of 75 – 150 μm sized UD root bark powder samples (Gel Film-1,2 and 3) showed higher swelling capacity than those made up of below 75 μm sized samples (Gel Film-4,5 and 6). Furthermore, the gel film containing 0.5 g of UD root bark powder sample (Gel Film-2) exhibited the highest swelling capacity (Qs: 11.2). The Gel Film-2 showed a 1.5-fold higher swelling capacity than Gel Film-5 (same contents of UD root bark, but different particle size) and a 7-fold higher value than the commercial Mediderm® hydrocolloid dressing. These results were in good accordance with the water absorption capacity data (Figure S2).

3.9. Bioadhesiveness study of UD gel films

The swelling of gel film by absorbing the fluids from the wound provides bioadhesiveness to the gel, allowing them to adhere to the wound site. This would be beneficial as physically masking the wound site provides a barrier to prevent any opportunistic infection. However, if the gel film binds too strongly to the wound, then it would be difficult to detach and also cause pain. This commonly occurs for many commercial wet dressings which generally possess great adhesiveness to the wound site. When compared with the commercial wet dressings, the UD gel films we developed exhibited a distinct advantage. As shown in Fig. 7, when the adhesion test was carried out with the prepared gel films on pigskin, unlike the Mediderm®, they showed differential adhesiveness

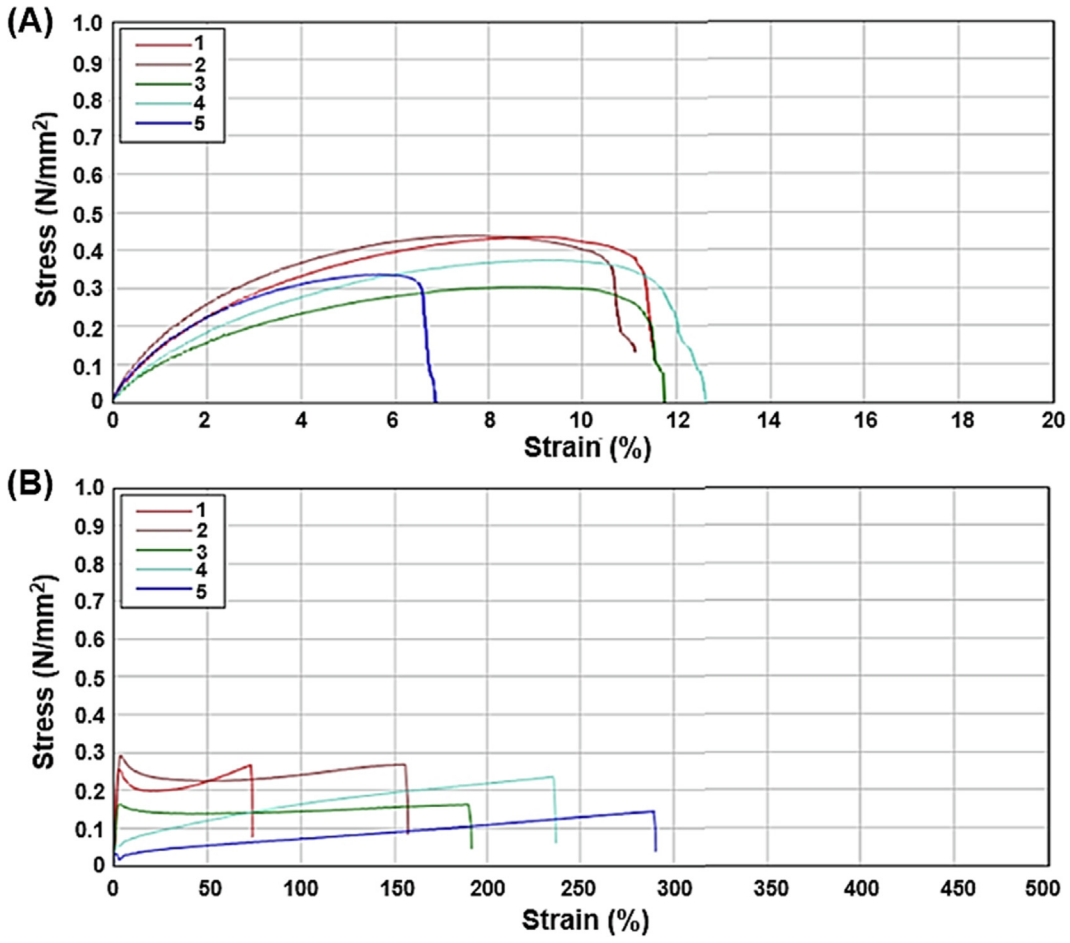

Fig. 5. Stress–strain curves for the (A) pullulan gel film and (B) UD gel film.

Table 2
Mechanical properties of UD gel films.

Samples	% Elongation	Tensile Strength (N/25.4 mm)
Gel Film-2	22.67 ± 4.05	12.91 ± 4.64
Gel Film-5	25.68 ± 3.45	4.78 ± 2.06

dependent upon the absence/presence of water. At dried condition, the gel films showed relatively weak adhesiveness, but when it was swollen by absorption of water, then the adhesiveness markedly increased similar to Mediderm®. These results suggested that, when applying the gel film to the wound site, after absorption of the exudates and then getting dried, the gel film could be easily detached. For both gel films composed of 75 – 150 μm sizedand below 75 μm sized samples, with lower glycerin content, greater adhesiveness change was observed.

3.10. Biocompatibility study

To verify the biocompatibility, the cytotoxicity of the leach-out products from the UD gel film was assessed by WST-1 assay. The viability of the cells incubated with the gel extracts is shown in Fig. 8. As seen, up to 50% extract little cytotoxicity, the cell viability was above 90% on both the cell types. These results for the gel leach-out extracts evidences the good tolerance of the gel film. Also, the hemo-biocompatibility was evaluated by the hemolytic study with mouse RBCs. Compared to the positive control group (1% Triton-X 100 solution), the UD gel film led to an insignificant level of RBC lysis (15.3 ± 2.3%) comparable to the PBS control group (12.7 ± 1.1%) after 24 h incubation. Overall, both studies evidenced that the UD gel film formulation is safe and biocompatible.

3.11. Effects of UD gel film on wound healing in mice

The wound healing effects of UD gel films were evaluated in ICR mice. For a total of 5 days, punctured wounds were differentially treated daily for each group (Fig. 9), and the wound contraction rate was assessed. The representative wound images of each group along time are shown in Fig. 10. As seen, the wounds treated with UD gel film showed a markedly faster rate of wound closure compared with other groups (Fig. 10A). At Day 1, the unclosed wound area of the UD gel film group was significantly decreased to 61.4%, while there was little difference in the wound size of other groups (control: 93.1%, control gel film: 84.5% and Madeca Band®: 92.4%) (Fig. 10B). On Day 6 when the study was terminated, the unclosed wound area of control, UD gel film, control gel film, and Madeca Band® treated groups were 48.4%, 25.6%, 32.9%, and 42.9%, respectively (Fig. 10C). Only the UD gel film-treated group showed a significant reduction in the wound size. Apart from accelerating the wound contraction rate, the UD gel film was able to dry the wound site and prevent potential contamination. Specifically, in the control group, despite applying the povidone-iodine disinfectant solution, some of the wounds of the control group got infected. Added to the wound healing efficacy, the UD gel films possessed another crucial advantage over other dressings. The UD gel film had a sharp difference in the adhesiveness when it was dried and wet. When applied to the wound site, after absorbing the exudates, the UD

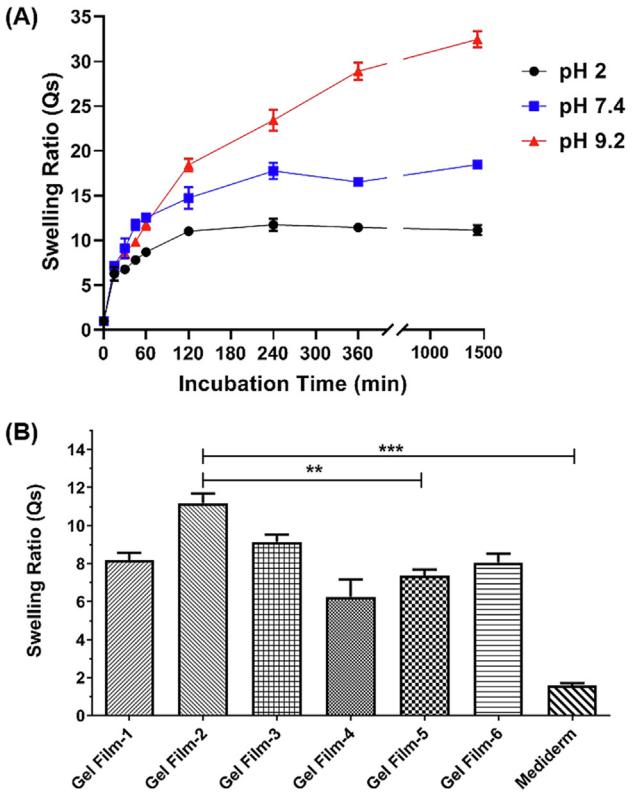

Fig. 6. Swelling properties of UD gel film. (A) Swelling kinetics of UD gel film (Gel Film-2) in different pH (2.0, 7.4, and 9.2). (B) Comparison of the swelling capacity of different UD gel film formulations in pH 7.4 simulated wound solutions after 1 h incubation. ***$p < 0.001$ and **$p < 0.01$ were displayed as statistical significance by 1-way ANOVA analysis with Tukey's multiple comparison test as the *post hoc* test.

gel film became highly adhesive and could firmly maintain on the wound site alone. However, once the gel film got dried, the adhesiveness significantly reduced, and it could be easily removed without causing pain. When compared with the UD gel film, the control gel film was disintegrated rapidly after applying to the wound site, and, for the most of the time during the study, the wound site was remained open. In contrast, the Madeca Band® adhered to the wound site firmly and was continuously

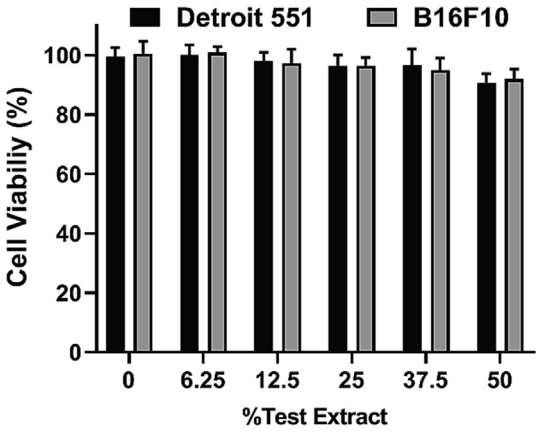

Fig. 8. Cytotoxicity study results for the leach-out products of the UD gel film on Detroit 551 human normal skin and B16F10 murine melanoma cell lines.

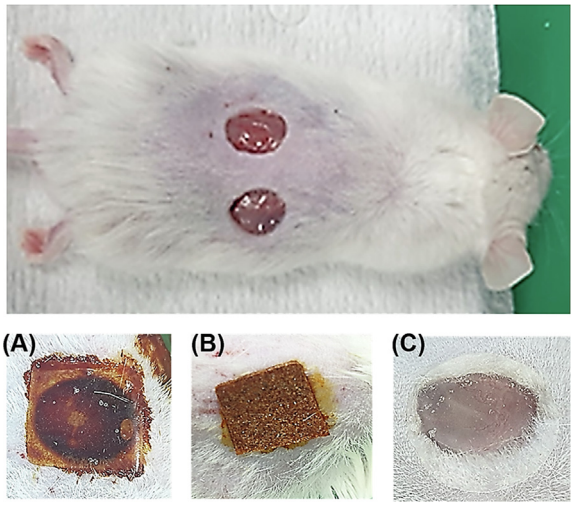

Fig. 9. Application of different gel film samples on skin wound mice model. The upper image is showing the wounds on the dorsal part of mice and the lower images are (A) control gel film, (B) UD gel film, and (C) Madeca Band® applied to the wound site.

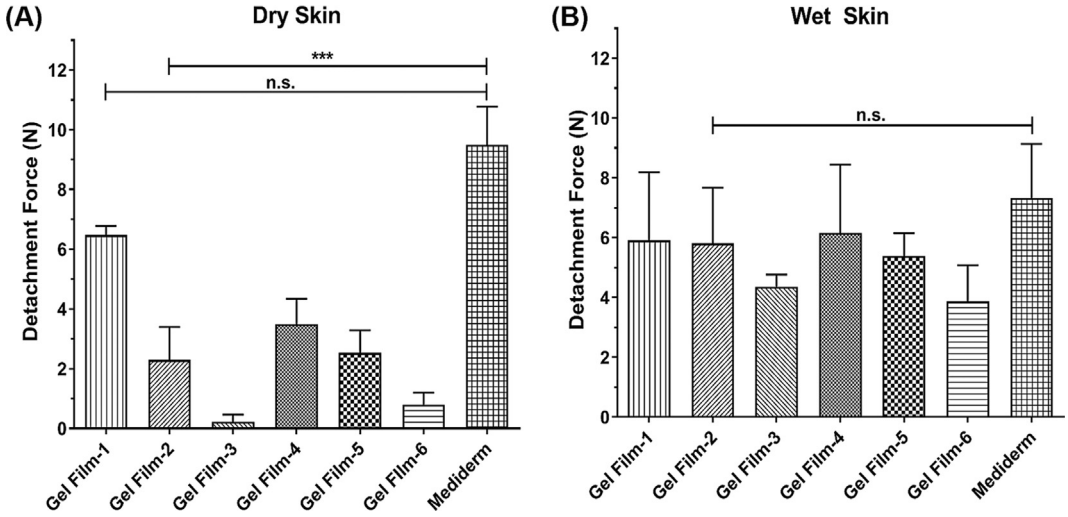

Fig. 7. Skin adhesiveness test results for UD gel films (no. 1–6) and Mediderm on (A) dry and (B) wet pigskin. ***$p < 0.001$ and n.s. (not significant) were displayed by 1-way ANOVA analysis with Tukey's multiple comparison test.

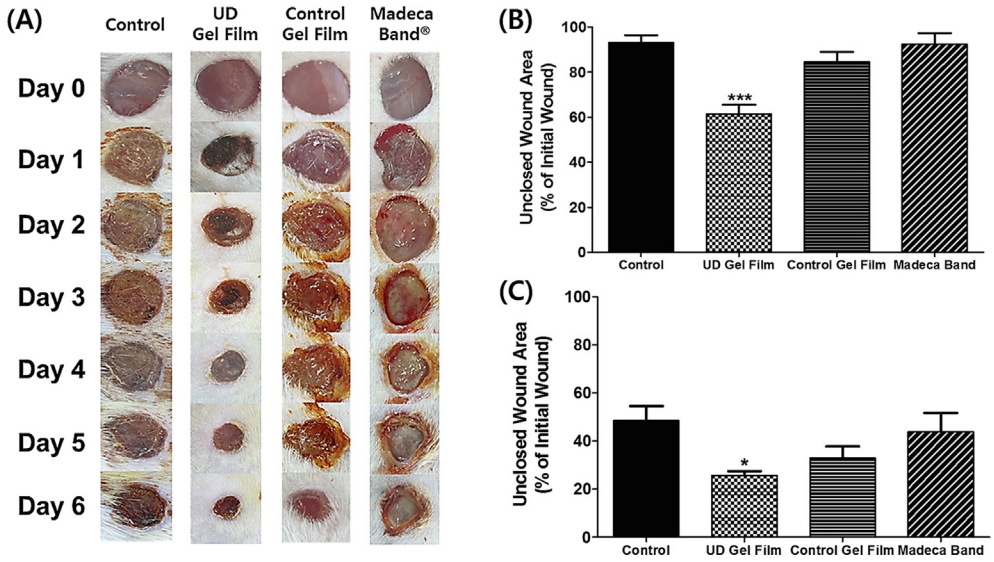

Fig. 10. Efficacy study results of gel film samples on skin wound mice model. The wound areas were compared for control mouse vs. applications of UD gel film, control gel film, or Madeca band: (A) The wound closure profiles from Day 0 to Day 6 and the unclosed wound area on Day 1 (B) and Day 6 (C).

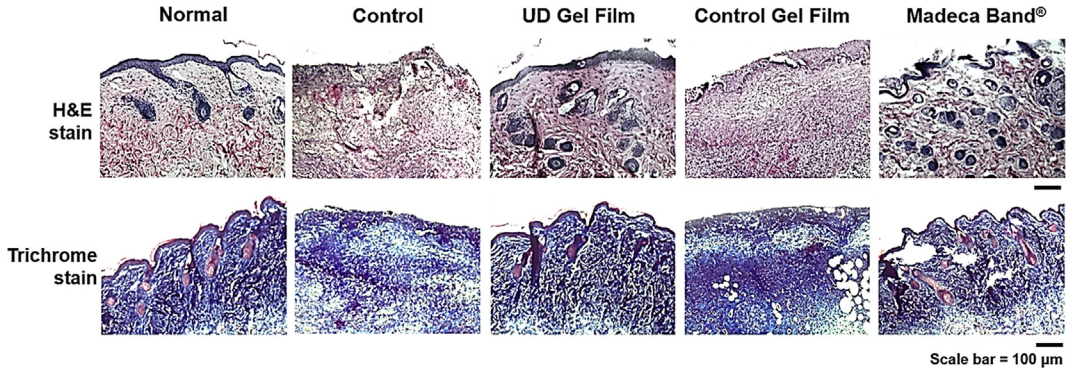

Fig. 11. Histology images of the skin wound tissues. The wound tissue was harvested on Day 6 when the efficacy study was terminated. The normal tissue and wound tissues from control mice vs. mice treated with gel films or Madeca band were fixed in formalin and underwent the H&E and Masson's trichrome staining procedures. Images of normal skin tissue vs. wound tissues were acquired with a light-contrast microscope.

maintained. The Madeca Band® had more difficulty to remove from the wound site than the UD gel film for replacement. As shown in Fig. 11, when the wound skins were further histologically analyzed after H&E and Masson's trichrome staining, the UD gel film-treated group showed markedly greater deposition of collagen in the dermis when compared with other groups, and, a faster rate of wound closure with the regeneration of the epidermis over the wound area. These results from the UD gel film-treated group were even superior to the positive control group treated with Madeca Band®; suggesting that UD gel films are potentially great candidates for use as wound dressings.

4. Conclusions

To date, many types of dressings are commercially available. However, there is yet no ideal products that could be effectively applied to specifically large wounds with high exudates such as diabetic foot ulcers and pressure sores. Thus, it is compelling to develop wound dressings specialized in such chronic wounds. In the present research, we developed a novel UD gel film composed of UD rook bark powders and evaluated its efficacy in a mice model. In previous studies, it has usually been the UD root bark extracts, not the original root bark powders that have been of research interest. However, in sharp contrast to the UD root bark extracts, the UD root bark powders possess distinct gelling activity and excellent gel swelling capacity which are mainly known to be the contribution of the mucilage compositions. This unique property makes the UD root bark powders a great material for hydrogel film dressing. Indeed, our study results confirmed that the UD gel films possessed a markedly higher capacity for absorbing water than commercial wet dressings and, when tested in a mice wound model, showed superior wound healing effects (faster wound closure and dermal regeneration) to control groups. Added to the wound healing efficacy, the differential adhesiveness dependent upon the dry/wet condition renders the UD gel films to be even superior wound dressings to others. Overall, this research demonstrated the applicability of UD root bark powders as a material for hydrogel wound dressings and the therapeutic potentials of UD gel films for effective wound healing.

Declarations of Competing Interest

None.

Acknowledgment

This work was financially supported by the R&D Program for Forest Science Technology (Project No. 2017036A00-1919-BA01) provided by the Korea Forest Service (Korea Forestry Promotion Institute).

Appendix A. Supplementary material

Supplementary data to this article can be found online at https://doi.org/10.1016/j.jsps.2020.05.007.

References

Adderley, U.J., 2010. Managing wound exudate and promoting healing. Br. J. Community. Nurs. 15 (Sup1), S15–S20. https://doi.org/10.12968/bjcn.2010.15.Sup1.46907.

Archana, G., Sabina, K., Babuskin, S., Radhakrishnan, K., Fayidh, M.A., Babu, P.A.S., Sivarajan, M., Sukumar, M., 2013. Preparation and characterization of mucilage polysaccharide for biomedical applications. Carbohydr. Polym. 98 (1), 89–94. https://doi.org/10.1016/j.carbpol.2013.04.062.

Behm, B., Babilas, P., Landthaler, M., Schreml, S., 2012. Cytokines, chemokines and growth factors in wound healing. J. Eur. Acad. Dermatol. Venereol. 26 (7), 812–820. https://doi.org/10.1111/j.1468-3083.2011.04415.x.

Bishop, S.M., Walker, M., Rogers, A.A., Chen, W.Y., 2003. Importance of moisture balance at the wound-dressing interface. J. Wound Care 12 (4), 125–128. https://doi.org/10.12968/jowc.2003.12.4.26484.

Bradford, C., Freeman, R., Percival, S.L., 2009. In vitro study of sustained antimicrobial activity of a new silver alginate dressing. J. Am. Coll. Certif. Wound Spec. 1 (4), 117–120. https://doi.org/10.1016/j.jcws.2009.09.001.

Braiman-Wiksman, L., Solomonik, I., Spira, R., Tennenbaum, T., 2007. Novel insights into wound healing sequence of events. Toxicol. Pathol. 35 (6), 767–779. https://doi.org/10.1080/01926230701584189.

Chen, C.T., Chen, K.I., Chiang, H.H., Chen, Y.K., Cheng, K.C., 2017. Improvement on physical properties of pullulan films by novel cross-linking strategy. J. Food Sci. 82 (1), 108–117. https://doi.org/10.1111/1750-3841.13577.

Collins, M.N., Birkinshaw, C., 2008. Physical properties of crosslinked hyaluronic acid hydrogels. J. Mater. Sci. - Mater. Med. 19 (11), 3335–3343. https://doi.org/10.1007/s10856-008-3476-4.

Dabiri, G., Damstetter, E., Phillips, T., 2016. Choosing a Wound Dressing Based on Common Wound Characteristics. Adv. Wound Care 5 (1), 32–41. https://doi.org/10.1089/wound.2014.0586.

Dhivya, S., Padma, V.V., Santhini, E., 2015. Wound dressings - a review. Biomedicine 5 (4), 22. https://doi.org/10.7603/s40681-015-0022-9.

Eaglstein, W.H., 2001. Moist wound healing with occlusive dressings: a clinical focus. Dermatol. Surg. 27 (2), 175–181. https://doi.org/10.1046/j.1524-4725.2001.00299.x.

Elzayat, E.M., Auda, S.H., Alanazi, F.K., Al-Agamy, M.H., 2018. Evaluation of wound healing activity of henna, pomegranate and myrrh herbal ointment blend. Saudi Pharm. J. 26 (5), 733–738. https://doi.org/10.1016/j.jsps.2018.02.016.

Gałka, P., Kowalonek, J., Kaczmarek, H., 2014. Thermogravimetric analysis of thermal stability of poly (methyl methacrylate) films modified with photoinitiators. J. Therm. Anal. Calorim. 115 (2), 1387–1394. https://doi.org/10.1007/s10973-013-3446-z.

Han, Y., Lv, S., 2019. Synthesis of chemically crosslinked pullulan/gelatin-based extracellular matrix-mimetic gels. Int. J. Biol. Macromol. 122, 1262–1270. https://doi.org/10.1016/j.ijbiomac.2018.09.080.

Hosgood, G., 2006. Stages of wound healing and their clinical relevance. Vet. Clin. North Am. Small Anim. Pract. 36 (4), 667–685. https://doi.org/10.1016/j.cvsm.2006.02.006.

Hussain, A., Samad, A., Singh, S., Ahsan, M., Haque, M., Faruk, A., Ahmed, F., 2016. Nanoemulsion gel-based topical delivery of an antifungal drug: in vitro activity and in vivo evaluation. Drug Deliv. 23 (2), 642–657. https://doi.org/10.3109/10717544.2014.933284.

Jones, D.S., 1999. Dynamic mechanical analysis of polymeric systems of pharmaceutical and biomedical significance. Int. J. Pharm. 179 (2), 167–178. https://doi.org/10.1016/S0378-5173(98)00337-8.

Jung, M.J., Heo, S.I., Wang, M.H., 2008. Free radical scavenging and total phenolic contents from methanolic extracts of Ulmus davidiana. Food Chem. 108 (2), 482–487. https://doi.org/10.1016/j.foodchem.2007.10.081.

Kang, M.C., Yumnam, S., Park, W.S., So, H.M., Kim, K.H., Shin, M.C., Ahn, M.-J., Kim, S.Y., 2020. Ulmus parvifolia accelerates skin wound healing by regulating the expression of MMPs and TGF-β. J. Clin. Med. 9 (1), 59. https://doi.org/10.3390/jcm9010059.

Kannon, G.A., Garrett, A.B., 1995. Moist wound healing with occlusive dressings: a clinical review. Dermatol. Surg. 21 (7), 583–590. https://doi.org/10.1111/j.1524-4725.1995.tb00511.x.

Kao, H.K., Chen, B., Murphy, G.F., Li, Q., Orgill, D.P., Guo, L., 2011. Peripheral blood fibrocytes: enhancement of wound healing by cell proliferation, re-epithelialization, contraction, and angiogenesis. Ann. Surg. 254 (6), 1066–1074. https://doi.org/10.1097/SLA.0b013e3182251559.

Kavousi, H.R., Fathi, M., Goli, S.A., 2017. Stability enhancement of fish oil by its encapsulation using a novel hydrogel of cress seed mucilage/chitosan. Int. J. Food Prop. 20, 1890–1900. https://doi.org/10.1080/10942912.2017.1357042.

Kim, D., Maharjan, P., Jin, M., Park, T., Maharjan, A., Amatya, R., Yang, J., Min, K.A., Shin, M.C., 2019. Potential albumin-based antioxidant nanoformulations for ocular protection against oxidative stress. Pharmaceutics 11 (7), 297. https://doi.org/10.3390/pharmaceutics11070297.

Lai, W.F., Rogach, A.L., 2017. Hydrogel-based materials for delivery of herbal medicines. ACS Appl. Mater. Interfaces 9 (13), 11309–11320. https://doi.org/10.1021/acsami.6b16120.

Leathers, T.D., 2003. Biotechnological production and applications of pullulan. Appl. Microbiol. Biotechnol. 62 (5–6), 468–473. https://doi.org/10.1007/s00253-003-1386-4.

Lee, G.Y., Jang, D.S., Kim, J., Kim, C.S., Kim, Y.S., Kim, J.H., Kim, J.S., 2008. Flavan-3-ols from Ulmus davidiana var. japonica with inhibitory activity on protein glycation. Planta Med. 74 (15), 1800–1802. https://doi.org/10.1055/s-0028-1088324.

Lee, M.K., Sung, S.H., Lee, H.S., Cho, J.H., Kim, Y.C., 2001. Lignan and neolignan glycosides from Ulmus davidiana var. japonica. Arch. Pharm. Res. 24 (3), 198–201. https://doi.org/10.1007/bf02978256.

Li, D.-X., Liu, B.-L., Liu, Y.-S., Chen, C.-L., 2008. Predict the glass transition temperature of glycerol–water binary cryoprotectant by molecular dynamic simulation. Cryobiol. 56 (2), 114–119. https://doi.org/10.1016/j.cryobiol.2007.11.003.

Ma, Y., Xin, L., Tan, H., Fan, M., Li, J., Jia, Y., Ling, Z., Chen, Y., Hu, X., 2017. Chitosan membrane dressings toughened by glycerol to load antibacterial drugs for wound healing. Mater. Sci. Eng., C 81, 522–531. https://doi.org/10.1016/j.msec.2017.08.052.

Nayak, A.K., Pal, D., Santra, K., 2014. Ispaghula mucilage-gellan mucoadhesive beads of metformin HCl: Development by response surface methodology. Carbohydr. Polym. 107, 41–50. https://doi.org/10.1016/j.carbpol.2014.02.022.

Ovington, L.G., 2007. Advances in wound dressings. Clin. Dermatol. 25 (1), 33–38. https://doi.org/10.1016/j.clindermatol.2006.09.003.

Pathare, Y.S., Hastak, V.S., Bajaj, A.N., 2013. Polymers used for fast disintegrating oral films: a review. Int. J. Pharm. Sci. Rev. Res. 21, 169–178.

Patil, S.C., Tagalpallewar, A.A., Kokare, C.R., 2019. Natural anti-proliferative agent loaded self-microemulsifying nanoparticles for potential therapy in oral squamous carcinoma. J. Pharm. Investig. 49 (5), 527–541. https://doi.org/10.1007/s40005-018-00415-x.

Phaechamud, T., Lertsuphotvanit, N., Issarayungyuen, P., Chantadee, T., 2019. Design, fabrication and characterization of xanthan gum/liquid-loaded porous natural rubber film. J. Pharm. Investig. 49 (1), 149–160. https://doi.org/10.1007/s40005-018-0396-2.

Raja, Sivamani, K., Garcia, M.S., Isseroff, R.R., 2007. Wound re-epithelialization: modulating keratinocyte migration in wound healing. Front. Biosci. 12, 2849–2868. https://doi.org/10.2741/2277.

Ridiandries, A., Tan, J.T.M., Bursill, C.A., 2018. The Role of Chemokines in Wound Healing. Int. J. Mol. Sci. 19 (10), 3217. https://doi.org/10.3390/ijms19103217.

Risbud, M.V., Bhonde, R.R., 2000. Polyacrylamide-chitosan hydrogels: in vitro biocompatibility and sustained antibiotic release studies. Drug Deliv. 7 (2), 69–75. https://doi.org/10.1080/107175400266623.

Seaman, S., 2002. Dressing selection in chronic wound management. J. Am. Podiatr. Med. Assoc. 92 (1), 24–33. https://doi.org/10.7547/87507315-92-1-24.

Sezer, A.D., Hatipoglu, F., Cevher, E., Oğurtan, Z., Bas, A.L., Akbuğa, J., 2007. Chitosan film containing fucoidan as a wound dressing for dermal burn healing: preparation and in vitro/in vivo evaluation. AAPS PharmSciTech 8 (2), E94–E101. https://doi.org/10.1208/pt0802039.

So, H.M., Yu, J.S., Khan, Z., Subedi, L., Ko, Y.-J., Lee, I.K., Park, W.S., Chung, S.J., Ahn, M.-J., Kim, S.Y., Kim, K.H., 2019. Chemical constituents of the root bark of Ulmus davidiana var. japonica and their potential biological activities. Bioorg. Chem. 91,. https://doi.org/10.1016/j.bioorg.2019.103145 103145.

Son, G.-H., Lee, H.-J., Na, Y.-G., Lee, H.-K., Kim, S.-J., Huh, H.-W., Kim, K.-T., Kang, J.-S., Kim, Y.-H., Myung, C.-S., Yoon, M.-H., Kim, S.J., Cho, H.S., Lee, J.-Y., Cho, C.-W., 2019. Formulation and statistical analysis of an herbal medicine tablet containing Morus alba leaf extracts. J. Pharm. Investig. 49 (6), 625–634. https://doi.org/10.1007/s40005-018-00417-9.

Teramoto, N., Shibata, M., 2006. Synthesis and properties of pullulan acetate. Thermal properties, biodegradability, and a semi-clear gel formation in organic solvents. Carbohydr. Polym. 63 (4), 476–481. https://doi.org/10.1016/j.carbpol.2005.10.008.

Ustundag Okur, N., Hokenek, N., Okur, M.E., Ayla, S., Yoltas, A., Siafaka, P.I., Cevher, E., 2019. An alternative approach to wound healing field; new composite films from natural polymers for mupirocin dermal delivery. Saudi Pharm. J. 27 (5), 738–752. https://doi.org/10.1016/j.jsps.2019.04.010.

Vuddanda, P.R., Montenegro-Nicolini, M., Morales, J.O., Velaga, S., 2017. Effect of plasticizers on the physico-mechanical properties of pullulan based pharmaceutical oral films. Eur. J. Pharm. Sci. 96, 290–298. https://doi.org/10.1016/j.ejps.2016.09.011.

Watts, C.R., Rousseau, B., 2012. Slippery elm, its biochemistry, and use as a complementary and alternative treatment for laryngeal irritation. Am. J. Physiol. Biochem. 1 (1), 17–23. https://doi.org/10.5455/jib.20120417052415.

Xu, X., Liu, X., Li, Q., Hu, J., Chen, Q., Yang, L., Lu, Y., 2017. New amphiphilic polycarbonates with side functionalized cholesteryl groups as biomesogenic units: synthesis, structure and liquid crystal behavior. RSC Adv. 7 (23), 14176–14185. https://doi.org/10.1039/c7ra00360a.

Yang, C., Xu, L., Zhou, Y., Zhang, X., Huang, X., Wang, M., Han, Y., Zhai, M., Wei, S., Li, J., 2010. A green fabrication approach of gelatin/CM-chitosan hybrid hydrogel for wound healing. Carb. Polym. 82 (4), 1297–1305. https://doi.org/10.1016/j.carbpol.2010.07.013.

Yeo, J.S., Seo, Y.H., Jung, C.H., Na, S.I., 2019. Structural design considerations of solution-processable graphenes as interfacial materials via a controllable synthesis method for the achievement of highly efficient, stable, and printable planar perovskite solar cells. Nanoscale 11 (3), 890–900. https://doi.org/10.1039/c8nr05698f.

Zhang, C., Gao, D., Ma, Y., Zhao, X., 2013. Effect of gelatin addition on properties of pullulan films. J. Food Sci. 78 (6), C805–C810. https://doi.org/10.1111/j.1750-3841.2012.02925.x.